JOURNAL OF MATERIALS SCIENCE 10 (1975) 1343–1350

Failure of brittle polymers by slow crack growth

Part 2 *Failure processes in a silica particle-filled epoxy resin composite*

R. J. YOUNG, P. W. R. BEAUMONT
Department of Engineering, University of Cambridge, UK

The variation of crack velocity (V) with stress intensity factor (K_I) at the tip of a crack has been measured for an epoxy resin containing 42% by volume of irregularly-shaped silica particles. It has been found that at crack velocities above 10^{-5} m sec^{-1} the crack propagates primarily through the silica particles, whereas at velocities below this value, failure occurs primarily by particle pull-out. This variation in fracture mode is accompanied by a corresponding change in slope of the $V(K)$ curve. Using data obtained from creep rupture experiments and the derived $V(K)$ relationship, it has been possible to estimate the size of the inherent flaw in the composite. This was found to be approximately twice the average particle diameter which is also equal to the size of the largest particles ($\sim$ 140 μm). Fracture of the unfilled epoxy resin and the effect of environment upon slow crack growth in the composite have also been investigated.

1. Introduction

Silica particles are added to epoxy resins for several reasons. They reduce the cost, degree of shrinkage, exothermic temperature rise and coefficient of thermal expansion, and increase the thermal conductivity. However, the addition of these particles also affects the mechanical properties of the material. In general, the stiffness of the silica particle-epoxy resin composite is higher than that of the pure epoxy resin [1] and also the composite normally has a higher fracture toughness than the unreinforced resin [2-4]. There is currently considerable interest in understanding the toughening mechanisms in brittle materials modified by the inclusion of second phase brittle particles [2-9]. Experimental work has centred upon measuring the toughness of the composite as a function of the particle volume fraction [2-5, 7, 9, 10] and surface treatment of the particles [4, 9, 10] during fast (unstable) crack propagation. In the present investigation we have studied slow (stable) crack growth in an epoxy resin containing 42% by volume silica particles where the surface treatment of the silica had been kept constant. This material has been found to suffer from subcritical crack growth and the variation of crack velocity (V) with stress intensity factor (K_I) at the tip of the crack has been measured using a double torsion (DT) specimen developed for brittle ceramics [11, 12]. This test enables the $V(K)$ relationship to be evaluated rapidly over a range of crack velocities between approximately 10^{-2} and 10^{-10} m sec^{-1} using a load relaxation technique that does not require direct observation of the moving crack. This approach has enabled microfailure processes in the composite to be studied as a function of crack velocity. By constructing $V(K)$ diagrams it has been possible to predict the times-to-failure of specimens loaded to stresses below those required to initiate fast catastrophic fracture; also a model has been proposed to explain the microscopic fracture behaviour of this kind of composite material. The DT specimen can be easily used in wet and dry environments and the effect of water upon crack propagation in the composite has also been studied.

2. Experimental

2.1. Materials and test conditions

The material investigated was a silica-filled

epoxy resin composite supplied in the form of 7 mm thick sheets by CIBA-GEIGY (UK) Ltd (Duxford). The epoxy resin was CT 200 cured with HT 901 hardener and filled with Z 300 silica flour*. This flour consisted of irregularly shaped silica particles and sieve analysis showed that over 50% of the particles were in the range 64 to 74 μm. The ratio of epoxy resin to hardener to filler was 100:30:200 parts by weight; densities of 1.23 g cm^{-3} for the epoxy resin and 2.65 g cm^{-3} for the silica gave a volume fraction of silica of about 42%. The composite had been cured at 135°C for 16 h. A sample of CT 200 epoxy resin cured under similar conditions with HT 901 hardener in the ratio of 100:30 parts by weight but without the silica flour was also examined.

Most tests were carried out in air at 20 ± 2°C with a relative humidity of 60 ± 10%. Some preliminary experiments were carried out to investigate the effect of environment using distilled water and paraffin both at 20 ± 2°C.

2.2. Specimen design and analysis

Double torsion (DT) specimens were machined from the sheets of material in the form of 75 mm by 30 mm rectangular plates. The specimens were edge-notched at one end and a V-shaped groove was machined from the notch along one face of each specimen. In the DT test, the sample is loaded as described in Part 1. It can be shown [11, 12] that the stress intensity factor (K_I) at the tip of the crack is independent of crack length and for an elastic material is given by

$$K_I = PW_m \left(\frac{3(1+\nu)}{Wt^3 t_n}\right)^{\frac{1}{2}} \quad (1)$$

where P is the applied load, W_m is the moment arm, ν is the Poisson's ratio of the material, W is the bar width, t is the plate thickness and t_n is the plate thickness in the plane of the crack.

2.3. Determination of crack velocity

It was shown in Part 1 that the crack velocity may be determined in one of three different ways. They are summarized below.

2.3.1. Direct observation

This method involves measuring the distance (Δa) that the crack has travelled, when the specimen is held on a constant load, P (or K_I). The crack velocity, V, is therefore equal to $(\Delta a/\Delta t)_P$.

*Hoben Davis Ltd.

2.3.2. Relaxation method

If the plate is loaded and held at a constant displacement ($dy/dt = 0$), the crack velocity is given by [11, 12]

$$V = \left(\frac{da}{dt}\right)_y = -\frac{P_{i,f}}{P^2}\left[a_{i,f} + C/B\right] \left(\frac{dP}{dt}\right)_y \quad (2)$$

where $P_{i,f}$ is the initial (or final) applied load, P is the instantaneous load, $a_{i,f}$ is the initial (or final) crack length and B and C are constants related to the slope and intercept of the compliance calibration curve, (y/P) $f(a)$, respectively.

2.3.3. Constant displacement rate method

If the DT specimen is loaded at a constant cross-head displacement rate (dy/dt) the crack will grow at constant load, P (or K_I). The crack velocity is simply related to the cross-head speed through the slope of the compliance calibration curve, such that [11, 12].

$$\left(\frac{dy}{dt}\right) = BP\left(\frac{da}{dt}\right) = BPV \quad (3)$$

For all of these methods, the value of K_I is calculated using Equation 1.

2.4. Procedure

The test device which was illustrated schematically in Part 1 was used in an Instron loading machine. In order to calculate K_I from Equation 1, we have assumed the Poisson's ratio (ν) of epoxy resin to be 0.25 and for the filled system ν has been taken as 0.27.

All three methods of measuring crack velocity were employed although most of the data was obtained using the load relaxation method. The analysis of this method described in Part 1 assumes that the load relaxation is due entirely to crack growth; however, in viscoelastic materials load relaxation will take place in the arms of the DT specimen because of the time-dependence of modulus. This would, therefore, give rise to an overestimate of the crack velocity. In the present investigation we have reduced this source of error by preloading the specimens to a value of K_I where the crack velocity was very low ($< 10^{-10}$ m sec^{-1}). The load is held constant for about 15 min to allow load relaxation in the

arms to take place. The specimen was then loaded at a cross-head speed of the order of 10 mm min^{-1} to a value of K_I where the crack growth rate was appreciable ($\sim 10^{-3}$ m sec^{-1}) and the load relaxation test continued in the manner described earlier. Since the composite contained about 42% by volume of silica particles, material relaxations were not particularly severe when compared with other glassy polymers such as PMMA. The load relaxation method permitted several experiments to be carried out upon the same specimen which tended to reduce the inherent scatter. The good agreement between the crack velocities measured using the load relaxation method and crack velocities obtained by the other two methods confirmed confidence in the load relaxation technique.

Evans [11] has pointed out that the apparent crack velocity in the DT specimen should be corrected by a small amount to take into account the curved nature of the crack front profile. This correction factor is equal to $b/(\Delta a^2 + b^2)^{\frac{1}{2}}$ where b is the width of the crack and Δa is the difference between the crack length, a, measured along the bottom and top surfaces of the DT specimen. For the filled epoxy resin specimens the factor was of the order of 0.4 and all the crack velocities quoted in this paper have been adjusted by this amount.

2.5. Fractography

Fracture surfaces of typical specimens were examined in a Stereoscan scanning electron microscope. The surfaces were prepared for observation by depositing thin layers ($\sim$ 100 Å) of carbon and gold-palladium alloy onto the fracture surfaces.

3. Results

3.1. Constant displacement-rate tests

The fracture of the unreinforced epoxy resin was investigated using the constant displacement-rate method. The material showed discontinuous cracking with the crack jumping at intervals through the specimen. Fig. 1a shows a load–time curve for the epoxy resin and the peak values of load correspond to values of K_{IC} of 0.85 $\pm$ 0.05 MN $m^{-3/2}$. Phillips and Scott [13] found similar behaviour for other types of epoxy resins fractured using the DT specimen; in some cases, however, they observed continuous cracking depending upon the curing cycle.

The load–time curves from constant displacement-rate tests on the composite were quite different from those obtained for the epoxy resin and showed continuous cracking (Fig. 1b). The load increased linearly at first before settling down at a constant load during continuous crack growth. The load finally decreased sharply only when the crack reached the end of the specimen. This behaviour was identical in both water and paraffin.

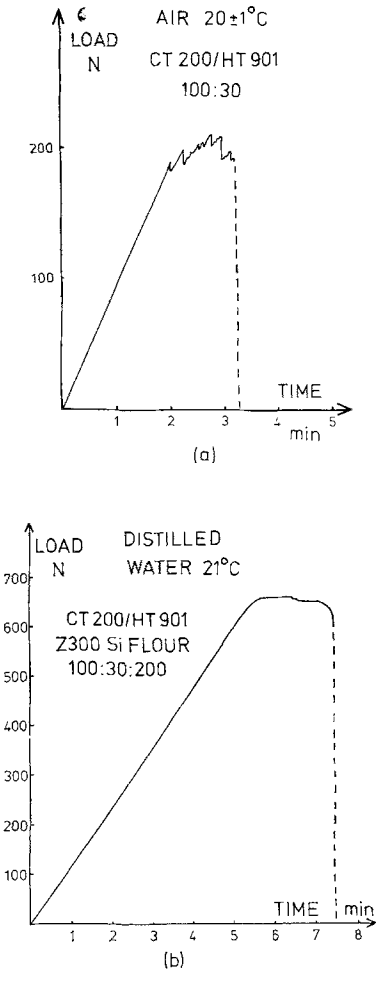

Figure 1 Load-time curves for double torsion specimens. (a) Epoxy resin in air; (b) filled resin in water.

3.2. $V(K)$ measurements

The relationship between V and K_I for the silica particle-filled epoxy resin in air is given in Fig. 2 in the form of a log-log plot. The data are mainly from load relaxation experiments and the symbols are explained in the figure caption. For the size of specimen used it was found that the

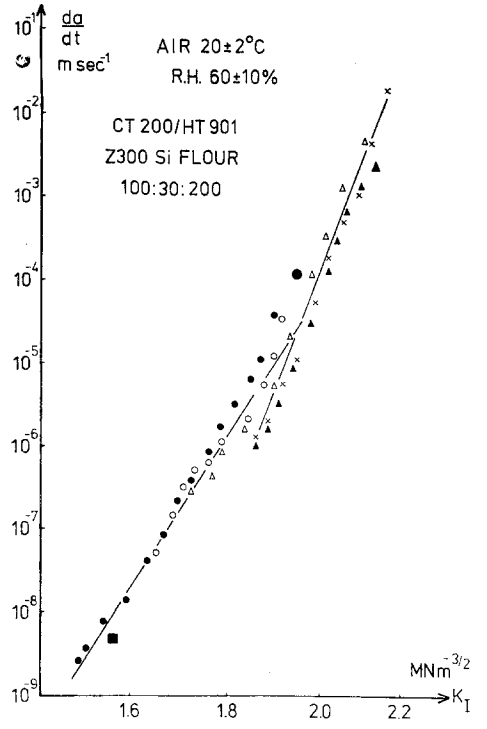

Figure 2 Crack velocity (da/dt) as a function of stress intensity factor (K_I) for the filled resin in air. The different symbols are from relaxation tests on different specimens. The three larger symbols are from constant displacement rate tests or direct measurements of crack velocity.

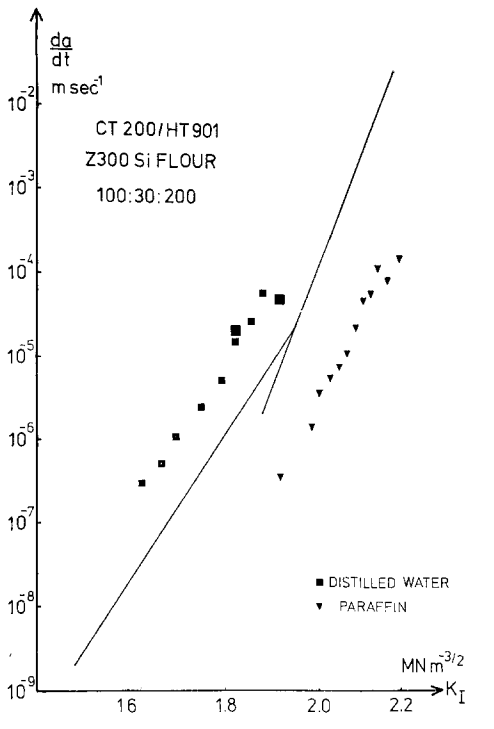

Figure 3 Crack velocity (da/dt) as a function of K_I for the filled resin in paraffin and distilled water measured using the relaxation method. The lines are taken from Fig. 2, and the larger symbols refer to constant displacement rate tests.

slope (B) and the intercept (C) of the compliance calibration curve were $1.0 \pm 0.1 \times 10^{-5}$ N^{-1} and $4.0 \pm 0.5 \times 10^{-4}$ mm N^{-1}, respectively. It can be seen that all the datum points fall approximately upon two intersecting straight lines. Above a crack velocity of about 10^{-5} m sec^{-1}, the $V(K)$ curve has a slope of about 60; below 10^{-5} m sec^{-1} the slope is lower at about 35. It must also be noted that over the range of K_I investigated there appears to be no threshold value of K_I (or K_I*) below which no crack growth occurred.

3.3. Environmental effects

Some preliminary experiments on slow crack growth in silica particle-filled epoxy resin in distilled water and paraffin were carried out using the DT specimen. The effect of environment upon the shape of the $V(K)$ diagram is shown in Fig. 3. The bimodal curve from Fig. 2 is also present with the datum points deleted. In water the crack velocities are increased by nearly one order of magnitude, whereas in paraffin the velocities are reduced by more than that amount. The effects of water and paraffin on slow crack growth in the composite are analogous to the effects they have on the fracture of pure glass [11, 12].

3.4. Microscopy

Fig. 4 is a photograph of the fracture surface of a DT specimen of the composite. In this area, two load relaxation tests have been carried out and the curved nature of the crack front can be seen. The arrow indicates the direction of crack growth. At the beginning of the test the fracture surface has a light appearance and as the crack slows down the surface becomes darker. It was found, from constant load and constant displacement rate tests using DT specimens, that the light surface was typical of areas where the crack velocity was greater than about 10^{-5} m sec^{-1}; at $V < 10^{-5}$ m sec^{-1} the surface took on a dark appearance. Fig. 5 shows Stereoscan photomicrographs of the two types of fracture surface. In the "fast" area ($V > 10^{-5}$ m sec^{-1})

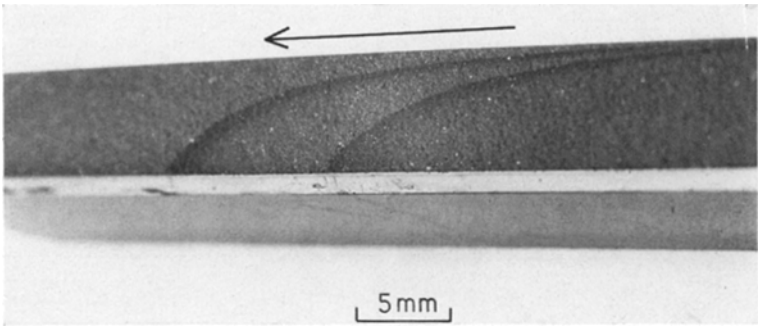

Figure 4 A fracture surface of the filled resin obtained in air. In the area shown, two relaxation tests have been carried out and the curved nature of the crack front can be seen. The arrow indicates the direction of crack growth.

it is difficult to differentiate between the silica particles and the epoxy resin since the crack appears to have propagated through both the filler and the matrix. In the "slow" area ($V < 10^{-5}$ sec^{-1}) the surface is much rougher and silica particles can be seen protruding from the fracture surface of the matrix. There are also gaps around the particles as a result of interfacial failure between the silica and the epoxy resin. This difference between "fast" and "slow" fracture can be considered analogous to transgranular and intergranular failure in metals.

A fracture surface of the pure epoxy resin examined at the same magnification as the surface of the composite appeared to be perfectly smooth.

4. Time-to-failure predictions

The relationship between V and K_I can be used to predict the life-time, ψ_f, of a component where ψ_f is controlled by subcritical (slow) crack growth. It has been shown that for the composite, V is a unique function of K_I at a given temperature and in a given environment.

The time-to-failure, ψ_f, at constant stress is given by the integral [11]

$$\psi_f = \int_{a_i}^{a_c} \frac{1}{V(K_I)}\, da \qquad (4)$$

where a_i is the initial crack size and a_c is the crack size at which the crack becomes unstable. Since

$$K_I = \sigma_a Y \sqrt{a}\,, \qquad (5)$$

where Y is a geometrical factor (equal to $\sqrt{\pi}$ for infinitely wide specimens) and σ_a is the applied stress, then

$$\psi_f = \frac{2}{\sigma_a^2 Y^2} \int_{K_{Ii}}^{K_{Ic}} \frac{K_I}{V(K_I)}\, dK_I\,, \qquad (6)$$

where K_{Ii} is the initial value of K_I and K_{Ic} is the value of K_I at which the crack becomes unstable,

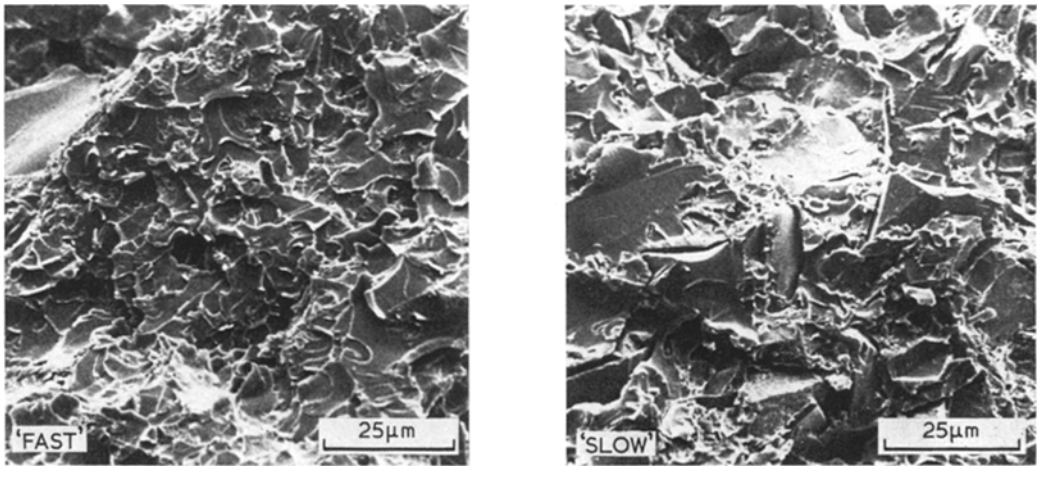

Figure 5 Scanning electron micrographs of a fracture surface of the filled epoxy resin obtained in air. In the "fast" area the crack was growing faster than about 10^{-5} m sec^{-1} and in the "slow" area the crack velocity was lower than this value.

normally called the plane strain fracture toughness of the material. Over the range of velocities measured, there does not seem to be a unique value of K_{IC} for unstable fracture. For the integral in Equation 6, we have taken K_{IC} as the highest measured value of K_I in Fig. 2. This corresponds to a velocity of the order of 10^{-1} m sec^{-1} and does not affect the value of the integral for times-to-failure of greater than 10^{-3} sec.

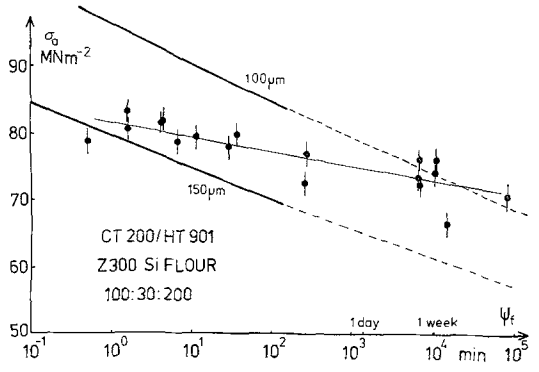

Figure 6 Creep rupture data for the filled resin at 22°C in air [14].The two heavy lines have been calculated from the measured $V(K)$ relationship in Fig. 2 using values of inherent flaw size of 100 and 150 μm. They have been extended with dashed lines by assuming that the $V(K)$ relationship can be extrapolated to velocities lower than those actually measured.

Fig. 6 gives experimentally measured time-to-failure values for unnotched tensile specimens of the composite held at various constant stress levels (σ_a) at 22°C [14]. The predicted times-to failure, ψ_f, have also been plotted in Fig. 6 for different values of a_i, the initial flaw size. It may be seen that, within experimental error, most of the measured values fall within the predictions for 100 μm $< a_i <$ 150 μm. However the slope of the measured data is significantly less than that of the predicted lines, indicating that the strength of the material does not fall off as rapidly as the prediction from the $V(K)$ measurements would imply. This prediction gives an underestimate of the specimen lifetime probably because it relies upon crack growth rate measurements at very low velocities ($\sim 10^{-8}$ m sec^{-1}) and an extrapolation of the $V(K)$ curve to even lower ones. It is clear, therefore, that an accurate knowledge of the $V(K)$ relationship at low velocities is required before time-to-failure predictions can be made with certainty in this material.

TABLE I Variation of fracture surface energy, γ_s, fracture toughness, K_{IC}, and Young's modulus, E, for the pure epoxy resin, the resin filled with silica flour and pure silica glass

	CT 200/ HT 901 [2]	CT 200/ HT 901 + 42% silica flour	Silica glass [15]
γ_s (J m^{-2})	120	250 ± 50	4.4
K_{IC} (MN m$^{-3/2}$)	0.86	2.2 ± 0.1	0.79
E (GN m^{-2})	3.1	10 ± 1	72

5. Discussion

5.1. Toughening mechanisms

Table I gives the fracture surface energy, γ_s, plane strain fracture toughness, K_{IC} and Young's modulus, E, for the pure resin [2], the composite investigated in this work and silica glass [14]. γ_s has been calculated for the composite using the relation

$$K_{IC} = \sqrt{\left[\frac{2E_c\gamma_s}{(1-\nu^2)}\right]} \quad (7)$$

under plane strain conditions. The Young's modulus of the composite, E_c, was calculated using the specimen dimensions and the slope of the compliance calibration curve (B) through the relation

$$E_c = \frac{6W_m^2(1+\nu)}{Wt^3B} \cdot \quad (8)$$

K_{IC} for the composite has again been taken as the highest measured value of K_I (Fig. 2). It is clear from Table I that the composite is tougher than either of the two components; γ_s for the filled system is about 250 J m^{-2} which is over twice that of the pure resin and sixty times that of silica glass.

Several research workers [2, 3, 6-9] have attempted to isolate the strengthening mechanisms in brittle solids filled with brittle second phase particles. Three main proposals have been put forward to explain this phenomenon:

(1) an increase in surface area due to crack branching that leads to an increase in the measured fracture surface energy;

(2) plastic deformation of the matrix around the second phase particles; and

(3) an increase in the line energy of the crack

front as a result of crack bowing due to pinning by the second phase obstacles. This is analogous to the "line tension effect" in dislocation pinning in metals.

Detailed investigation of these mechanisms has been carried out by varying the volume fraction and particle size [2-10]. It seems from these investigations that there is no one universal toughening mechanism for all composite systems. Clearly, the first mechanism must increase the measured value of γ_s and this effect must always be present when the fracture surface of the composite is rougher than that of the pure material. However, it is doubtful that this mechanism alone can account for the measured increase in γ_s [3]. It is known that under certain conditions, materials that are thought to be brittle will undergo plastic deformation. Glass, for example, will flow under a hardness indenter [15] and epoxy resins yield and flow in compression tests [16]. Lilley [2] considered that in epoxy resins filled with second phase particles, local plastic deformation around the particles was responsible for the increase in γ_s, and he discounted the third mechanism. By varying volume fraction and particle size, Lange [7] showed that in a sodium borosilicate glass–Al_2O_3 system the increase in γ_s could be more satisfactorily explained by considering the interaction of the crack front with the second phase dispersion, although there was also an increase in γ_s because of surface roughness. Evans [8] showed that increases in strength would be expected for a brittle matrix containing second phase brittle particles because of a "line tension effect". He showed this effect would be important at high volume fractions (i.e. small interparticle spacings).

5.2. Microfailure processes

An important feature brought to light in this present work is the dependence of fracture behaviour of the composite on the crack velocity and environment. The microfailure processes at the crack tip in the composite may be affected by a localized concentration of a chemical species (such as moisture) in the environment. The chemical species can, therefore, influence the failure processes by affecting (1) plastic deformation in the epoxy resin, (2) surface energy of the silica particles and epoxy resin and (3) interfacial bond energy between the silica and matrix. However, there are no available data at present to establish whether or not water vapour in the atmosphere has influenced these surface energy terms to any great extent. It can only be suggested that water may have affected these surface energy terms and interfacial bond energy to the extent that the mode of crack propagation is a function of the rate of reaction and crack velocity.

5.2.1. Crack velocity and environmental effects

The $V(K)$ diagram for the silica-epoxy resin composite shows the overall crack growth rate is composed of at least two elementary microfailure processes composed of transparticle and interparticle fracture. At $V > 10^{-5}$ m sec^{-1} failure occurs by fracture through the silica particles and the curve has a slope (n) of about 60; at $V < 10^{-5}$ m sec^{-1} crack propagation occurs by particle-matrix debonding and particle pull-out, and the slope (n) of the curve is about 35. The overall rate of crack growth will, therefore, be determined by an activation energy spectrum for the overall reaction between the composite and moisture in the environment. This activation energy spectrum may exhibit discrete values each associated with one of the specific rate-controlling elementary reactions or breakdown of the silica-epoxy resin interface. At the intersection of these two curves at $V_T = 10^{-5}$ m sec^{-1} (Fig. 2), the individual rates of reaction between environment and silica, or environment and interface, are equal; elsewhere, one step will have a rate significantly different to the other. The overall crack propagation rate in the composite will, therefore, depend on the reaction kinetics of the overall reaction between material and environment.

It is highly likely that the transition between transparticle fracture and interparticle failure will be affected by surface treatment of the silica particles. If the particle–matrix bond is strengthened, the pulling out of particles should be inhibited; with a weak bond particle fracture should not occur. A strong bond should, therefore, improve the long term properties where crack velocities are low ($< 10^{-5}$ m sec^{-1}); conversely, weakly-bonded particles should increase the impact resistance of the composite where crack velocities are greater than 10^{-5} m sec^{-1}

5.3. Inherent flaw size

The strength of a structural material is governed by the size of the largest inherent flaw that exists in the component. Analysis of the time-to-failure

data in Section 4 has shown that the critical inherent flaw size (a_0) in the unnotched creep rupture specimens was of the order of 100 to 150 μm. We must now consider what microstructural features would give rise to flaws of this size. In the silica-filled epoxy resin, over 50% of the particles are between 64 and 74 μm in diameter, although it is known that particles greater than this size do exist. The interparticle spacing, d, can be estimated from the equation [3]

$$d = \frac{2D(1 - V_f)}{3V_f} \quad (9)$$

where D is the average particle diameter and V_f is the volume fraction of silica in the composite. For a composite with V_f equal to 0.42 and D equal to 70 μm, $d = 65$ μm which corresponds to about one half of the average size of the predicted inherent flaws. It is known that a range of particle sizes and, therefore, a distribution of interparticle spacings exists in the composite. From these simple estimations of inherent flaw size we can only conclude at the present time that a_0 is equivalent to the largest: (1) cracks in the matrix between particles, (2) fractured particles, or (3) silica particles debonded by interfacial failure. An increase in the strength of the composite should, therefore, be obtained by reducing the average silica particle size and interparticle spacing in the composite.

6. Conclusions and implications

Previous investigations into the fracture behaviour of composite materials consisting of brittle second phase particles in a brittle matrix have shown that the fracture behaviour of the composite is affected by composition, particle size and particle surface treatment. This present investigation has shown that the behaviour is also affected by crack velocity and environment. It has been found that the crack velocity (V) is a unique function of the stress intensity factor (K_I) at the tip of the crack. In water the crack velocity is increased by a factor of eight, whereas in paraffin the velocity is reduced by over one order of magnitude.

Two distinct failure mechanisms have been identified. In air at crack velocities in excess of 10^{-5} m sec^{-1} failure takes place mainly by means of particle fracture; at crack velocities below this value, failure takes place primarily by interfacial breakdown and particle pull-out. This change in failure mechanism is accompanied by a transition in the $V(K)$ diagram at about 10^{-5} m sec^{-1}. Using the $V(K)$ relationship and time-to-failure data obtained from creep rupture experiments, it has been possible to estimate the size of the inherent flaws present in the composite to be 100 to 150 μm.

Acknowledgements

We are grateful to Mr Graham Hodgetts of CIBA-GEIGY (UK) Limited (Duxford) for providing us with the material and the creep rupture data. One of us (R.J.Y.) would like to thank the Master and Fellows of St. John's College, Cambridge for support in the form of a Research Fellowship.

References

1. K. C. RADFORD, *J. Mater. Sci.* **6** (1971) 1286.
2. J. LILLEY, Ph.D. Thesis, University of Keele (1973).
3. F. F. LANGE and K. C. RADFORD, *J. Mater. Sci.* **6** (1971) 1197.
4. L. J. BROUTMAN and S. SAHU, *Mater. Sci. Eng.* **8** (1971) 98.
5. D. P. H. HASSELMAN and R. M. FULRATH, *J. Amer. Ceram. Soc.* **49** (1966) 68.
6. F. F. LANGE, *Phil. Mag.* **22** (1970) 983.
7. *Idem, J. Amer. Ceram. Soc.* **54** (1971) 614.
8. A. G. EVANS, *Phil. Mag.* **27** (1972) 1327.
9. J. C. HAMMOND and D. V. QUALE, Paper presented at Churchill Conference on "Yield Deformation and Fracture of Polymers", Cambridge (1973).
10. A. WAMBACH, K. TRACHTE and A. DIBENEDETTO, *J. Comp. Mater.* **2** (1968) 266.
11. A. G. EVANS, *J. Mater. Sci.* **7** (1972) 1137.
12. *Idem, Int. J. Fract.* **9** (1973) 267.
13. D. C. PHILLIPS and J. M. SCOTT, *J. Mater. Sci.* **9** (1974) 1202.
14. CIBA-GEIGY (UK) Limited, unpublished work.
15. S. M. WIEDERHORN, *J. Amer. Ceram. Soc.* **52** (1969) 99.
16. P. B. BOWDEN and J. A. JUKES, *J. Mater. Sci.* **7** (1972) 52.

Received 31 December1974 and accepted 13 January 1975